Inorg. Chem. **2008**, *47*, 8813−8822

Synthesis, Structure, and Spectroscopic Properties of Chiral Oxorhenium(V) Complexes Incorporating Polydentate Ligands Derived from L-Amino Acids: A Density Functional Theory/Time-Dependent Density Functional Theory Investigation

Sucharita Basak and Kajal Krishna Rajak*

Inorganic Chemistry Section, Department of Chemistry, Jadavpur University, Kolkata, 700 032, India

Received April 29, 2008

The oxorhenium(V) complexes $[Re^{V}O(L_A)Cl_2]$ bearing the (N-2-pyridylmethyl) of L-valine (HL_A^1), L-leucine (HL_A^2), and L-phenylalanine (HL_A^3) and $[Re^{V}O(L_B)Cl]$ containing the {(N-2pyridylmethyl)-(N-(5-nitro-2-hydroxybenzyl)} of L-valine ($H_2L_B^1$), L-leucine ($H_2L_B^2$), and L-phenylalanine ($H_2L_B^3$) are presented in this article. The complexes are isolated in enantiomeric pure form examined from X-ray structure determination. The complexes are characterized by spectroscopic and electrochemical methods. The molecular structures observed in the solid state are grossly preserved in solution (^1H, ^{13}C, and circular dichroism spectra). Gas-phase geometry optimization and the electronic structures of $[Re^{V}O(L_A^1)Cl_2]$, $[Re^{V}O(L_A^2)Cl_2]$, and $[Re^{V}O(L_B^2)Cl]$ have been investigated with the framework of density functional theory. The absorption and circular dichroism spectra of the complexes were also calculated applying time-dependent density functional theory (TDDFT) using the conductor-like polarizable continuum solvent model to understand the origin of the electronic excitations. The chemical shift (^1H and ^{13}C) as well as $^1H-^1H$ spin−spin coupling constant were also computed by the gauge-independent atomic orbital method, and the computed values are consistent with the experimental data.

Introduction

The chemistry of oxorhenium(V) complexes incorporating O,N coordinating ligands is of abiding interest.[1−7] In this context, the chemistry of enantiomeric pure chiral oxorhenium(V) complexes derivatized of α amino acids or small peptides has received a great deal of attention in recent years.[8−14] These demand further investigation of the underlying chemistry of the enantiomeric pure chiral oxorhenium(V) complexes incorporating O,N-coordinating polydentate ligands derived from optically active α amino acids.

In this paper, we wish to report a series of chiral oxorhenium(V) complexes as in **1** and **2** with the conformationally labile NNO and NONO coordinating ligands containing α amino acids such as L-valine, L-leucine, and L-phenylalanine. The complexes are characterized by IR,

* Author to whom correspondence should be addressed. E-mail: kkrajak@chemistry.jdvu.ac.in, kajalrajak@hotmail.com.

(1) (a) Morrill, C.; Grubbs, R. H. *J. Am. Chem. Soc.* **2005**, *127*, 2842. (b) Cai, Y.; Espenson, J. H. *Inorg. Chem.* **2005**, *44*, 2560.
(2) Ison, E. A.; Trivedi, E. R.; Corbin, R. A.; Abu-Omar, M. M. *J. Am. Chem. Soc.* **2005**, *127*, 15374.
(3) Chakraborty, I.; Panda, B. K.; Gangopadhyay, J.; Chakravorty, A. *Inorg. Chem.* **2005**, *44*, 1054.
(4) (a) Benny, P. D.; Green, J. L.; Engelbrecht, H. P.; Barnes, C. L.; Jurisson, S. S. *Inorg. Chem.* **2005**, *44*, 2381. (b) Belangar, S.; Beauchamp, A. L. *Inorg. Chem.* **1997**, *36*, 3640.
(5) (a) Dilworth, J. R.; Griffiths, D. V.; Parroti, S. J.; Zheng, Y. J. *J. Chem. Soc., Dalton. Trans.* **1997**, 2931. (b) Marzilli, L. G.; Banaszczyk, M. G.; Hansen, L.; kuklenyik, Z.; Cini, R.; Taylor, A., Jr. *Inorg. Chem.* **1994**, *33*, 4850.
(6) Libson, K.; Helm, L.; Roodt, A.; Cutler, C.; Merbach, A. E.; Sullivan, J.; Deutch, E. In *Technetium and Rhenium in Chemistry and Nuclear Medicine*; Nicolini, M., Bandoli, G., Mazzi, U., Eds.; Raven Press: New York, 1989; Vol. *3*.
(7) Schwerdtfeger, P.; Bast, R. *J. Am. Chem. Soc.* **2004**, *126*, 1652.
(8) Tessier, C.; Rochon, F. D.; Beauchamp, A. L. *Inorg. Chem.* **2004**, *43*, 7463.
(9) Melian, C.; Kremer, C.; Suescun, L.; Mombru, A.; Mariezcurrena, R.; Kremer, E. *Inorg. Chim. Acta* **2000**, *306*, 70.
(10) Liu, S.; Edwards, D. *Chem. Rev.* **1999**, *99*, 2235.
(11) Kirsch, S.; Jankowsky, R.; Leibnitz, P.; Spies, H.; Johannsen, B. J. *Biol. Inorg. Chem.* **1999**, *4*, 48.
(12) Kunze, S.; Zobi, F.; Kurz, Ph.; Spingler, B.; Alberto, R. *Angew. Chem.* **2004**, *43*, 5025.
(13) Benhaim, S.; Kahn, D.; Weiner, G. J.; Madsen, M. T.; Waxman, A. D.; Williams, C. M.; Clarkepearson, D. L.; Coleman, R. E.; Maguire, R. T. *Nucl. Med. Biol.* **1994**, *21*, 131.
(14) Chatterjee, M.; Achari, B.; Das, S.; Banerjee, R.; Chakrabarti, C.; Dattagupta, J. K.; Banerjee, S. *Inorg. Chem.* **1998**, *37*, 5424.

10.1021/ic800764n CCC: $40.75
Published on Web 08/27/2008

UV−vis, NMR (^{1}H and ^{13}C), and circular dichroism (CD) spectroscopic techniques. X-ray structures of the selected complexes have been determined. The electrochemical behavior is also examined.

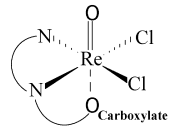

1

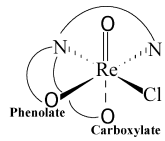

2

Here, we also present a full density functional theory (DFT) and time-dependent density functional theory (TD-DFT) investigation to get better insight into the geometry, electronic structure, and optical properties of these systems. Geometry optimizations of the singlet ground-state were carried out by means of DFT calculations. TDDFT calculations of several singlet states have been performed for better understanding of the electronic origin of the absorption and CD spectra. The computational modeling of the NMR parameter is also of abiding interest, and such calculation at DFT has emerged as a promising approach for the prediction of nuclear shielding and coupling constants of NMR active nuclei.[15] Thus, we have computed the proton and carbon NMR chemical shifts and also the ^{1}H−^{1}H spin−spin coupling constant using the gauge-independent atomic orbital (GIAO)−DFT method, which is aimed at providing the definitive characterization of the complexes.

Experimental Section

Materials. $(NBu_4)[ReOCl_4]$[16] and $[ReOCl_3(Me_2S)(OPPh_3)]$[17] were prepared as reported in the literature. All of the solvents were purified by standard procedures. All other chemicals were analytically pure and were used without further purification. All of the reactions were carried out under a dinitrogen atmosphere.

Physical Measurements. UV−vis spectra were measured on a Perkin-Elmer LAMBDA 25 spectrophotometer. IR spectra were recorded with Perkin-Elmer L-0100 spectrophotometer. ^{1}H and ^{13}C NMR spectral measurement were carried out on a Bruker FT 300 MHz spectrometer with tetramethylsilane (TMS) as an internal reference. The atom-numbering scheme used for ^{1}H NMR is the same as that used in crystallography and in Chart 1. Electrochemical measurements were performed (acetonitrile solution) on a CHI 620A electrochemical analyzer using a platinum electrode under a dinitrogen atmosphere. Tetraethylammonium perchlorate was used as a supporting electrolyte, and the potentials are referenced to the standard calomel electrode (SCE) without junction correction. The cyclic voltammograms were recorded with a scan rate of 50 mV/sec with *iR* compensation in all cases. Microanalyses (C, H, N) were obtained from a Perkin-Elmer 2400 Series II elemental analyzer. CD spectra were recorded on a JASCO-815 polarimeter.

Chart 1

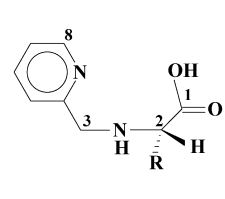

HL_A

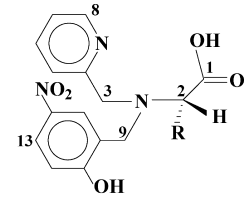

H_2L_B

R	HL_A	H_2L_B
$CHMe_2$	HL_A^1	$H_2L_B^1$
$CH_2(HCMe_2)$	HL_A^2	$H_2L_B^2$
CH_2Ph	HL_A^3	$H_2L_B^3$

Computational Details. The program package Gaussian 03W was employed for quantum mechanical calculations.[18] Ground-state electronic structure calculations of the selected complexes have been carried out using the DFT[19] method. Becke's three-parameter hybrid exchange functional[20] with the Lee−Yang−Parr (LYP) nonlocal correlation functional[21] was used throughout the computational study. A LANL2DZ[22] basis set along with the corresponding pseudopotential[23] was used for the rhenium atom in all calculations. The geometries of chiral oxorhenium(V) complexes were optimized in the gas phase without any symmetry constraint with the 6-31G basis set for H and the 6-31+G(d)[24a] basis set for C, N, O, and Cl atoms. The self-consistent field "tight" option of the Gaussian 03W program was used in all calculations to ensure sufficient convergence of the state energy values. Vibrational frequencies were calculated to ensure that the optimized geometries represent the local minima in all cases.

TDDFT[25] calculations in solution usually provide the excitation spectra and were performed in acetonitrile solution using the conductor-like polarizable continuum model[26] (CPCM) with larger basis set 6-311+G(d,p)[24b] for N, O, and Cl and 6-31+G(d,p) for C and H. We computed the lowest 40 singlet−singlet transitions.

(15) (a) Wolinski, K.; Hinton, J. F.; Pulay, P. *J. Am. Chem. Soc.* **1990**, *112*, 8251. (b) Taehtinen, P.; Bagno, A.; Klika, K.; Pihlaja, K. *J. Am. Chem. Soc.* **2003**, *125*, 4609. (c) Cloran, F.; Carmichael, I.; Serianni, A. S. *J. Am. Chem. Soc.* **2001**, *123*, 4781.
(16) Artus, G.; Abram, U.; Kaden, T. A. *J. Organomet. Chem.* **1995**, *492*, 217.
(17) Grove, D. E.; Wilkinson, G. *J. Chem. Soc.* **1966**, 1224.
(18) Frisch, M. J.; Trucks, G. W.; Schlegel, H. B.; Scuseria, G. E.; Robb, M. A.; Cheeseman, J. R.; Montgomery, J. A., Jr.; Vreven, T.; Kudin, K. N.; Burant, J. C.; Millam, J. M.; Iyengar, S. S.; Tomasi, J.; Barone, V.; Mennucci, B.; Cossi, M.; Scalmani, G.; Rega, N.; Petersson, G. A.; Nakatsuji, H.; Hada, M.; Ehara, M.; Toyota, K.; Fukuda, R.; Hasegawa, J.; Ishida, M.; Nakajima, T.; Honda, Y.; Kitao, O.; Nakai, H.; Klene, M.; Li, X.; Knox, J. E.; Hratchian, H. P.; Cross, J. B.; Ammi, R.; Pomelli, C.; Ochterski, J. W.; Ayala, P. Y.; Morokuma, K.; Voth, G. A.; Salvador, P.; Dannenberg, J. J.; Zakrzewski, V. G.; Dapprich, S.; Daniels, A. D.; Strain, M. C.; Farkas, O.; Malick, D. K.; Rabuck, A. D.; Raghavachari, K.; Foresman; J. B.; Ortiz, J. V.; Cui, Q.; Baboul, A. G.; Clifford; S.; Cioslowski, J.; Stefanov, B. B.; Liu; G.; Liashenko; A.; Piskorz, P.; Komaromi; I.; Martin; R. L.; Fox; D. J.; Keith, T.; Al-Laham, A.; Peng, C. Y.; Nanayakkara, A.; Challacombe, M.; Gill, P. M. W.; Johnson, B.; Chen, W.; Wong, M. W.; Gonzalez, C.; Pople, J. A. *Gaussian 03*, revision C.02; Gaussian, Inc.: Wallingford, CT, 2004.
(19) Parr, R. G.; Yang, W. *Density Functional Theory of atoms and molecules*; Oxford University Press: Oxford, U.K., 1989.
(20) Becke, A. D. *J. Chem. Phys.* **1993**, *98*, 5648.
(21) Lee, C.; Yang, W.; Parr, R. G. *Phys. Rev. B: Condens. Matter Mater. Phys.* **1988**, *37*, 785.
(22) Dunning, T. H.; Hay, P. J. In *Modern Theoritical Chemistry*; Schaefer, H. F., III, Ed; Plenum: New York, *3* (1976) 1
(23) Hay, P. J.; Wadt, W. R. *J. Chem. Phys.* **1985**, *82*, 299.
(24) (a) Schaefer, A.; Horn, H.; Ahlrichs, R. *J. Chem. Phys.* **1992**, *97*, 2571. (b) Schaefer, A.; Huber, C.; Ahlrichs, R. *J. Chem. Phys.* **1994**, *100*, 5829.
(25) (a) Bauernschmitt, R.; Ahlrichs, R. *Chem. Phys. Lett.* **1996**, *256*, 454. (b) Stratmann, R. E.; Scuseria, G. E.; Frisch, M. J. *J. Chem. Phys.* **1998**, *109*, 8218. (c) Casida, M. E.; Jamoroski, C.; Casida, K. C.; Salahub, D. R. *J. Chem. Phys.* **1998**, *108*, 4439.

In addition, the ^{1}H and ^{13}C NMR properties of the complexes were calculated with the magnetic field perturbation method with the GIAO algorithm[27] with the NMR = spin−spin keyword incorporated in the Gaussian 03W program. In calculation, the 6-311+G(2d,p) basis set was employed for all atoms other than rhenium. The relative chemical shift of a given nucleus X in the molecule was defined as δ_X^{calc} [ppm] = $\sigma_X^{ref} - \sigma_X^{calc}$ where TMS was used as a reference molecule optimized at the same level of theory.[27c,28a] In order to account for the solvent effect, we used the integral equation−formalism polarizable continuum model (IEF-PCM) method.[28b,c]

Crystallographic Studies. Single crystals of suitable quality for X-ray diffraction studies of the complexes [Re^{V}O(L$_A^1$)Cl$_2$], **1a**; [Re^{V}O(L$_A^2$)Cl$_2$], **1b**; and [Re^{V}O(L$_B^2$)Cl], **2b** were grown by slow evaporation of their acetonitrile solution. The X-ray intensity data were measured at 293 K on a Bruker-Nonious SMART APEX CCD diffractometer (Mo Kα, λ = 0.71073 Å). The detector was placed at a distance of 6.0 cm from the crystal. A total of 606 frames were collected with a scan width of 0.3° at different settings of φ.

The data were reduced in SAINTPLUS,[29] and empirical absorption correction was applied using the SADABS package.[29] Metal atoms were located from Patterson maps, and the rest of the non-hydrogen atoms emerged from successive Fourier synthesis. The structures were refined by a full-matrix least-squares procedure on F^2. All non-hydrogen atoms were refined anisotropically for **1a** and **2b**, and in the case of **1b**, few carbon atoms are refined isotropically. The hydrogen atom attached to an amine nitrogen atom for **1a** was directly located in different Fourier maps. The remaining hydrogen atoms in all cases were included in calculated positions. For **2b**, a large electron density value near the rhenium atom (_refine_diff_density_max 2.439) was located at the end of the refinement cycle. Calculations were performed using the SHELXTL v.6.14 program package.[30] Molecular structure plots were drawn using ORTEP.[31] Relevant crystal data are given in Table 1.

Synthesis of Complexes. The complexes [Re^{V}O(L$_A$)Cl$_2$] and [Re^{V}O(L$_B$)Cl] were prepared by using a general method with [ReOCl$_3$(Me$_2$S)(OPPh$_3$)] and (NBu$_4$)[ReOCl$_4$] as starting materials, respectively. Details are given below for one representative case (**1a** and **2a**).

[Re^{V}O(L$_A^1$)Cl$_2$], 1a. To 100 mg (0.15 mmol) of [ReOCl$_3$(Me$_2$S)-(OPPh$_3$)] in 25 mL of dichloromethane was added 48 mg (0.225 mmol) of the ligand (HL$_A^1$). The reaction solution was stirred at room temperature for 10 h, with precipitation of a sky-blue solid observed slowly over the course of the reaction. The solid was isolated by filtration. The product was recrystallized from a hot acetonitrile solution. Yield: 52 mg (70%). Anal. calcd for $C_{11}H_{15}N_2O_3Cl_2Re$: C, 27.50; H, 3.13; N, 5.83. Found: C, 27.28; H, 2.96; N, 5.79. UV−vis (λ_{max}/nm (ε/M^{-1} cm^{-1}) CH$_3$CN): 215 (18270), 280 (12020), 352 (2440), 710 (125). CD (λ_{max}/nm ($\Delta\varepsilon$/M^{-1} cm^{-1}) CH$_3$CN): 218 (+24.0), 280 (+11.0), 353 (−11.0), 700 (+0.15). IR$_{exptl}$ (KBr, cm^{-1}): ν(Re−Cl) 302, 315; ν(CO$_2$ sym) 1305; ν(CO$_2$ asym) 1686; ν(Re═O) 975. IR$_{calcd}$ (KBr, cm^{-1}): ν(Re−Cl) 312, 320; ν(CO$_2$ sym) 1293; ν(CO$_2$ asym) 1780; ν(Re═O) 1019. ^{1}H NMR$_{exptl}$ (δ (ppm), J (Hz), CD$_3$CN): 9.45 (H8, d, J = 5.27), 8.30−8.00 (ArH, 3H), 5.50 (H$_A$3, d, J = 16.10), 5.40 (N*H*), 5.10 (H$_B$3, d, J = 16.12), 3.35 (H2, m), 2.50 (H9, m), 0.95 and 0.80 (2C*H*$_3$, d, J = 5.40). ^{1}H NMR$_{calcd}$ (δ (ppm), J (Hz)): 9.90 (H8, d, J = 5.61), 8.85−8.30 (ArH, 3H), 5.75 (H$_A$3, d, J = 16.41), 4.90 (N*H*), 4.85 (H$_B$3), 3.25 (H2, m), 2.50 (H9), 1.10 and 1.05 (2C*H*$_3$, d, J = 5.20). ^{13}C NMR$_{exptl}$ (δ (ppm), CD$_3$CN): 174.5 (C1), 163.8 (C4), 152.2−124.2 (ArC, 4C), 73.4 (C2), 72.7 (C3), 30.0 (C9), 18.4 (C10), 18.3 (C11). ^{13}C NMR$_{calcd}$ (δ (ppm)): 183.0 (C1), 162.8 (C4), 153.0−132.0 (ArC, 4C), 79.0 (C2), 66.8 (C3), 35.4 (C9), 20.8 (C10), 19.7 (C11). E_{pa} (Re^V/Re^{VI} couple): 1.38 V (irr.)

[Re^{V}O(L$_A^2$)Cl$_2$], 1b. Yield: 55 mg (72%). Anal. calcd for $C_{12}H_{17}N_2O_3Cl_2Re$: C, 29.12; H, 3.44; N, 5.66. Found: C, 29.08; H, 3.36; N, 5.47. UV−vis (λ_{max}/nm (ε/M^{-1} cm^{-1}) CH$_3$CN): 218 (17560), 268 (11790), 351 (2405), 706 (130). CD (λ_{max}/nm ($\Delta\varepsilon$/M^{-1} cm^{-1}) CH$_3$CN): 220 (+25.5), 275 (+14.7), 357 (−12.3), 697 (+0.20). IR$_{exptl}$ (KBr, cm^{-1}): ν(Re−Cl) 316, 310; ν(CO$_2$ sym) 1320; ν(CO$_2$ asym) 1660; ν(Re═O) 975. IR$_{calcd}$ (KBr, cm^{-1}): ν(Re−Cl) 321, 310; ν(CO$_2$ sym) 1292; ν(CO$_2$ asym) 1782; ν(Re═O) 1019. ^{1}H NMR$_{exptl}$ (δ (ppm), J (Hz), CD$_3$CN): 9.55 (H8, d, J = 5.61), 8.20−7.90 (ArH, 3H), 5.40 (H$_A$3, d, J = 16.41), 5.15 (N*H*), 5.10 (H$_B$3, d, J = 16.50), 3.45 (H2, m), 2.10 (H9, m), 1.35 (H10), 1.00 and 0.75 (2C*H*$_3$, d, J = 5.20). ^{1}H NMR$_{calcd}$ (δ (ppm), J (Hz)): 9.80 (H8, d, J = 5.62), 8.85−8.30 (ArH, 3H), 5.70 (H$_A$3, d, J = 16.53), 5.25 (N*H*), 4.80 (H$_B$3), 3.70 (H2), 2.30 (H9), 1.40 (H10), 1.15 and 0.85 (2C*H*$_3$, d, J = 4.98). ^{13}C NMR$_{exptl}$ (δ (ppm), CD$_3$CN): 180.3 (C1), 160.6 (C4), 156.0−135.0 (ArC, 4C), 71.6 (C3), 70.0 (C2), 41.7 (C9), 29.3 (C10), 22.5 (C11), 19.0 (C12). ^{13}C NMR$_{calcd}$ (δ (ppm)): 184.7 (C1), 162.6 (C4), 152.1−131.0 (ArC, 4C), 73.4 (C3), 71.0 (C2), 43.1 (C9), 30.7 (C10), 24.4 (C11), 20.4 (C12). E_{pa} (Re^V/Re^{VI} couple): 1.33 V (irr.)

[Re^{V}O(L$_A^3$)Cl$_2$], 1c. Yield: 64 mg (78%). Anal. calcd for $C_{15}H_{15}N_2O_3Cl_2Re$: C, 34.09; H, 2.84; N, 5.30. Found: C, 34.08; H, 2.32; N, 4.99. UV−vis (λ_{max}/nm (ε/M^{-1} cm^{-1}) CH$_3$CN): 221 (22890), 265 (14470), 355 (5210), 715 (140). CD (λ_{max}/nm ($\Delta\varepsilon$/M^{-1} cm^{-1}) CH$_3$CN): 224 (+31.2), 270 (+26.8), 357 (−14.5), 702 (+0.20). IR (KBr, cm^{-1}): ν(Re−Cl) 308, 315; ν(CO$_2$ sym) 1312; ν(CO$_2$ asym) 1670; ν(Re═O) 972. ^{1}H NMR$_{exptl}$ (δ (ppm), J (Hz),

Table 1. Crystal Data and Structure Refinement Parameters for Complexes [Re^{V}O(L$_A^1$)Cl$_2$], [Re^{V}O(L$_A^2$)Cl$_2$], and [Re^{V}O(L$_B^2$)Cl]

	[Re^{V}O(L$_A^1$)Cl$_2$]	[Re^{V}O(L$_A^2$)Cl$_2$]	[Re^{V}O(L$_B^2$)Cl]
formula	$C_{11}H_{15}Cl_2N_2O_3Re$	$C_{12}H_{17}Cl_2N_2O_3Re$	$C_{19}H_{21}ClN_3O_6Re$
fw	480.35	494.38	609.04
cryst syst	monoclinic	triclinic	orthorhombic
space group	$P2(1)$	$P1$	$P2_12_12_1$
a (Å)	6.7537(14)	6.7488(13)	6.407(5)
b (Å)	10.797(2)	11.358(2)	14.418(5)
c (Å)	10.748(2)	11.931(2)	26.265(5)
α (deg)	90.00	115.53(3)	90.00(5)
β (deg)	107.85(3)	98.35(3)	90.00(5)
γ (deg)	90.00	94.26(3)	90.00(5)
V (Å^3)	746.0(2)	806.8(3)	2426(2)
Z	2	2	4
D_{calcd} (mg m^{-3})	2.139	2.035	1.667
μ (mm^{-1})	8.506	7.868	5.154
θ (deg)	1.99−26.01	1.93−28.27	1.55−25.99
T (K)	293(2)	293(2)	293(2)
R1,[a] wR2[b] [$I > 2\sigma(I)$]	0.0288, 0.0727	0.0355, 0.0779	0.0580, 0.1333
GOF on F^2	1.054	1.042	1.095

[a] R1 = $\sum||F_o| - |F_c||/\sum|F_o|$. [b] wR2 = $[\sum w(F_o^2 - F_c^2)^2/\sum w(F_o^2)^2]^{1/2}$.

(26) (a) Cossi, M.; Rega, N.; Scalmani, G.; Barone, V. J. *Comput. Chem.* **2003**, *24*, 669. (b) Cossi, M.; Barone, V. J. *Chem. Phys.* **2001**, *115*, 4708. (c) Barone, V.; Cossi, M. *J. Phys. Chem. A* **1998**, *102*, 1995.

(27) (a) Wolniski, K.; Hinton, J. F.; Pulay, P. *J. Am. Chem. Soc.* **1990**, *112*, 8251. (b) Dodds, J. L.; Mcweeny, R.; Sadlej, A. J. *Mol. Phys.* **1980**, *41*, 1419. (c) Ditchfield, R. *Mol. Phys.* **1974**, *27*, 789. (d) Mcweeny, R. *Phys. Rev.* **1962**, *126*, 1028. (e) London, F. *J. Phys. Radium* **1937**, 397.

(28) (a) Rohlfing, C. M.; Allen, L. C.; Ditchfield, R. *Chem. Phys.* **1984**, *8*, 9. (b) Cossi, M.; Barone, V.; Mennucci, B.; Tomasi, J. *Chem. Phys. Let.* **1998**, *286*, 253. (c) Cances, M. T.; Mennucci, B.; Tomasi, J. *J. Chem. Phys.* **1997**, *107*, 3032.

(29) *SMART*; *SAINT*; *SADABS*; *XPREP*; *SHELXTL*; Bruker AXS Inc.: Madison, WI, 1998.

(30) Sheldrick, G. M. *SHELXTL*, v. 6.14; Bruker AXS Inc.: Madison, WI, 2003.

(31) Johnson, C. K. *ORTEP Report ORNL-5138*; Oak Ridge National Laboratory: Oak Ridge, TN, 1976.

CD_3CN): 9.25 (H8, d, $J = 5.10$), 8.80−7.30 (ArH, 8H), 6.20 (H_A3, d, $J = 16.02$), 6.00 (H_B3, d, $J = 14.25$), 4.85 (N*H*), 3.10 (H2, m), 1.75 (H9, m).^{13}C NMR_{exptl} (δ (ppm), CD_3CN): 179.3 (C1), 164.3 (C4), 159.0−125.0 (ArC, 8C), 73.5 (C3), 71.2 (C2), 42.9 (C9). E_{pa} (Re^V/Re^{VI} couple): 1.31 V (irr.)

[$Re^VO(L_B^1)Cl$], 2a. A 66 mg (0.17 mmol) amount of $H_2L_B^1$ was added to a solution of 100 mg (0.17 mmol) of $[NBu_4][ReOCl_4]$ in 20 mL of dry ethanol. The reaction mixture was refluxed for 8 h, producing a green precipitate. It was then filtered, and the solid mass was then dissolved in a minimum volume of dichloromethane and subjected to column chromatography on a silica gel column (12 × 1 cm, 60−120 mesh). The green band was eluted using a benzene−acetonitrile (5:1) mixture. The green solid was obtained after removal of the solvent from the eluate under reduced pressure. Yield: 80 mg (75%). Anal. calcd for $C_{18}H_{19}N_3O_6ClRe$: C, 36.30; H, 3.19; N, 7.05. Found: C, 36.47; H, 3.23; N, 7.35. UV−vis (λ_{max}/nm (ε/M^{-1} cm^{-1}) CH_3CN): 216 (19405), 270 (11270), 354 (4995), 685(134). CD (λ_{max}/nm ($\Delta\varepsilon/M^{-1}$ cm^{-1}) CH_3CN): 224 (+27.4), 275 (−20.7), 370 (−15.9), 680 (+0.25). IR (KBr, cm^{-1}): ν(Re−Cl) 310; $\nu(CO_2$ sym) 1318; $\nu(CO_2$ asym) 1660; ν(Re═O) 980. ^{1}H NMR_{exptl} (δ (ppm), J (Hz), DMSO-d_6): 8.90 (H8, d, $J = 5.85$), 8.30−7.10 (ArH, 6H), 6.30 (H_A3, d, $J = 15.98$), 5.95 (H_B3, d, $J = 14.26$), 5.20 (H_A9, d, $J = 15.85$), 4.90 (H_B9, d, $J = 14.02$), 3.35 (H2, m), 1.70 (H16, m), 0.85 and 0.58 (2CH_3, d, $J = 5.90$). ^{13}C NMR_{exptl} (δ (ppm), DMSO-d_6): 178.9 (C1), 171.6 (C11), 163.8 (C4), 151.8−124.5 (ArC, 8C), 144.2 (C14), 72.7 (C3), 71.0 (C9), 64.8 (C2), 38.3 (C16), 21.8 (C17), 20.0 (C18). $E_{1/2}$ (Re^V/Re^{VI} couple): 1.45 V (ΔE_p, 85 mV).

[$Re^VO(L_B^2)Cl$], 2b. Yield: 83 mg (80%). Anal. calcd for $C_{19}H_{21}N_3O_6ClRe$: C, 37.43; H, 3.44; N, 6.89. Found: C, 37.25; H, 3.38; N, 6.36. UV−vis (λ_{max}/nm (ε/M^{-1} cm^{-1}) CH_3CN): 214 (19880), 270 (12480), 352 (4570), 690 (125). CD (λ_{max}/nm ($\Delta\varepsilon/M^{-1}$ cm^{-1}) CH_3CN): 220 (+28.6), 280 (−18.3), 368 (−16.1), 650 (+0.30). IR_{exptl} (KBr, cm^{-1}): ν(Re−Cl) 312; $\nu(CO_2$ sym) 1315; $\nu(CO_2$ asym) 1656; ν(Re═O) 978. IR_{calcd} (KBr, cm^{-1}): ν(Re−Cl) 299; $\nu(CO_2$ sym) 1312; $\nu(CO_2$ asym) 1792; ν(Re═O) 1003. ^{1}H NMR_{exptl} (δ (ppm), J (Hz), DMSO-d_6): 9.20 (H8, d, $J = 5.34$), 8.40−7.30 (ArH, 6H), 6.55 (H_A3, d, $J = 16.22$), 6.35 (H_B3, d, $J = 14.46$), 5.10 (H_A9, d, $J = 16.23$), 5.00 (H_B9, d, $J = 14.41$), 3.50 (H2, m), 1.85 (H16, m), 1.64 (H17, m), 0.90 and 0.55 (2CH_3, d, $J = 6.3$). ^{1}H NMR_{calcd} (δ (ppm), J (Hz)): 9.90 (H8, d, $J = 5.48$), 9.00−7.90 (ArH, 6H), 5.90 (H_A3, d, $J = 15.55$), 5.40 (H_B3, d), 5.20 (H_A9, d, $J = 14.53$), 5.05 (H_B9, d), 3.10 (H2), 1.87 (H16), 1.75 (H17), 0.90 and 0.55 (2CH_3, d, $J = 5.70$). ^{13}C NMR_{exptl} (δ (ppm), DMSO-d_6): 176.7 (C1), 173.6 (C11), 163.4 (C4), 154.8−121.6 (ArC, 8C), 145.1 (C14), 73.4 (C3), 72.6 (C9), 65.8 (C2), 39.2 (C16), 33.7 (C17), 25.4 (C18), 24.0 (C19). ^{13}C NMR_{calcd} (δ (ppm)): 180.0 (C1), 177.4 (C11), 162.9 (C4), 154.9−120.0 (ArC, 8C), 148.2 (C14), 74.4 (C3), 72.4 (C9), 66.2 (C2), 39.9 (C16), 33.6 (C17), 24.0 (C18), 21.3 (C19). $E_{1/2}$ (Re^V/Re^{VI} couple): 1.48 V (ΔE_p, 90 mV).

[$Re^VO(L_B^3)Cl$], 2c. Yield: 83 mg (76%). Anal. calcd for $C_{22}H_{19}N_3O_6ClRe$: C, 41.12; H, 2.96; N, 6.54. Found: C, 41.73; H, 3.05; N, 6.81. UV−vis (λ_{max}/nm (ε/M^{-1} cm^{-1}) CH_3CN): 225 (17790), 277 (12045), 361 (8120), 668 (105). CD (λ_{max}/nm ($\Delta\varepsilon/M^{-1}$ cm^{-1}) CH_3CN): 228 (+30.4), 260 (−15.3), 368 (−12.6), 670 (+0.30). IR (KBr, cm^{-1}): ν(Re−Cl) 308; $\nu(CO_2$ sym) 1320; $\nu(CO_2$ asym) 1665; ν(Re═O) 990. ^{1}H NMR_{exptl} (δ (ppm), DMSO-d_6): 9.20 (H8, d, $J = 4.80$), 8.60−7.10 (ArH, 11H), 6.57 (H_A3, d, $J = 15.74$), 5.90 (H_B3, d, $J = 13.90$), 5.20 (H_A9, d, $J = 15.32$), 5.00 (H_B9, d, $J = 13.94$), 3.30 (H2, m), 1.54 (H16, m). ^{13}C NMR_{exptl} (δ (ppm), DMSO-d_6): 176.7 (C1), 173.6 (C11), 163.0 (C4), 162.0−116.0 (ArC, 14C), 145.6 (C14), 74.0 (C3), 73.6 (C9), 69.1 (C2), 39.2 (C16). $E_{1/2}$ (Re^V/Re^{VI} couple): 1.50 V (ΔE_p, 90mV).

Result and Discussion

Synthesis. The chiral oxorhenium(V) complexes were synthesized with NNO and NONO coordinating α amino acid ligands. The NNO coordinating (N-2-pyridylmethyl) of L-valine, L-leucine, and L-phenylalanine (HL_A^1−HL_A^3, general abbreviation HL_A) as well as the NONO coordinating {(N-2-pyridylmethyl)-(N-(5-nitro-2-hydroxybenzyl)} of L-valine, L-leucine, and L-phenylalanine ($H_2L_B^1$−$H_2L_B^3$, general abbreviation H_2L_B) are used in the present work (Chart 1). The ligands are synthesized following the reported procedure.[32,33]

The $[Re^VO(L_A)Cl_2]$ complexes were obtained as a sky-blue solid in good yield from a reaction of $[ReOCl_3(Me_2S)(OPPh_3)]$ with HL_A in a ratio of 1:1.5 in a dichloromethane solution.

$$[Re^VOCl_3(Me_2S)(OPPh_3)] \xrightarrow[CH_2Cl_2]{HL_A} [Re^VO(L_A)Cl_2]$$

The stoichiometric reaction of $[NBu_4][Re^VOCl_4]$ with the tetradentate ligand (H_2L_B) in boiling ethanol afforded the green-colored complexes of the general formula $[Re^VO(L_B)Cl]$ in good yields.

$$[Re^VOCl_4]^- \xrightarrow[EtOH]{H_2L_B} [Re^VO(L_B)Cl]$$

IR Spectra. The IR spectra of the complexes were recorded in a KBr disk. The calculated IR spectra of three representative complexes are reported. The characteristic IR data are given in the Experimental Section.

The Re═O stretching frequency of the complexes occurs as a strong band in the region 960−980 cm^{-1} as compared to the calculated value of ∼1020 cm^{-1}. Carboxylate monocoordination[34] indicates the presence of symmetric (∼1300 cm^{-1}) and asymmetric (∼1670 cm^{-1}) stretching modes and that of modes calculated at ∼1290 and ∼1790 cm^{-1}, respectively. The $[Re^VO(L_B)Cl]$ complex displays a Re−Cl stretch near 310 cm^{-1}, whereas $[Re^VO(L_A)Cl_2]$ complexes show two well-resolved stretches at 315 and 305 cm^{-1} corresponding to the presence of a cis choloro group. The calculated Re−Cl frequencies span the range of 299−320 cm^{-1}. Therefore, despite some under- and overestimation of the calculated value, the values obtained are in agreement with the experimental results.

Crystal Structures. The molecular structures of $[Re^VO(L_A^1)Cl_2]$, **1a**; $[Re^VO(L_A^2)Cl_2]$, **1b**; and $[Re^VO(L_B^2)Cl]$, **2b** have been determined by single-crystal X-ray diffracto-

(32) Ceccato, A. S.; Neves, A.; Brito, M. A.; Drechsel, S. M.; Mangrich, A. S.; Werner, R.; Hasse, W.; Bortoluzzi, A. J. *J. Chem. Soc., Dalton Trans.* **2000**, 1573.
(33) Iikura, H.; Nagata, T. *Inorg. Chem.* **1998**, *37*, 4702.
(34) (a) Basak, S.; Mondal, A.; Chopra, D.; Rajak, K. K. *Polyhedron* **2007**, *26*, 3465. (b) Mondal, S.; Rath, S. P.; Rajak, K. K.; Chakravorty, A. *Inorg. Chem.* **1998**, *37*, 1713.

Table 2. Selected Bond Lengths [Å] and Angles [deg] for $[Re^{V}O(L_A^1)Cl_2]$, **1a**, and $[Re^{V}O(L_B^2)Cl]$, **2b**

	1a	2b		1a	2b
			Lengths		
Re1−O1	2.019(7)	2.001(7)	Re1−N2	2.136(11)	2.111(10)
Re1−O3	1.685(9)	1.674(7)	Re1−Cl1	2.319(3)	2.341(3)
Re1−O4		1.993(7)	Re1−Cl2	2.342(3)	
Re1−N1	2.176(8)	2.169(8)			
			Angles		
O1−Re1−N1	76.1(3)	77.1(3)	O3−Re1−O4		99.0(4)
O1−Re1−N2	80.3(3)	85.1(4)	O4−Re1−N1		96.3(4)
O1−Re1−Cl1	90.3(3)	91.5(2)	O4−Re1−N2		167.7(4)
O1−Re1−Cl2	88.6(2)		O4−Re1−Cl1		85.1(3)
O1−Re1−O3	162.9(4)	166.2(3)	N1−Re1−N2	78.0(4)	77.8(4)
O1−Re1−O4		83.1(4)	N1−Re1−Cl1	165.4(2)	168.3(2)
O3−Re1−N1	87.9(4)	89.0(3)	N1−Re1−Cl2	96.66(19)	
O3−Re1−N2	90.6(4)	91.7(4)	N2−Re1−Cl1	94.7(4)	98.6(3)
O3−Re1−Cl1	105.0(4)	102.3(3)	N2−Re1−Cl2	168.6(2)	
O3−Re1−Cl2	99.3(3)	99.0(4)	Cl1−Re1−Cl2	88.09(15)	

metry. The complexes crystallize in the $P2(1)$, $P1$, and $P2_12_12_1$ space groups, respectively. In all cases, the amino acid residue retains the *S* configuration.

The selected bond distances and angles for **1a** and **2b** are listed in Table 2, and the molecular views are shown in Figures 1 and 3, respectively. For **1b**, two metrically similar but crystallographically distinct molecules constitute the asymmetric unit. One of the molecules (molecule 1) is shown in Figure 2, and the selected bond parameters are given in the Supporting Information (Table S1). For the numbering scheme of **1b**, the

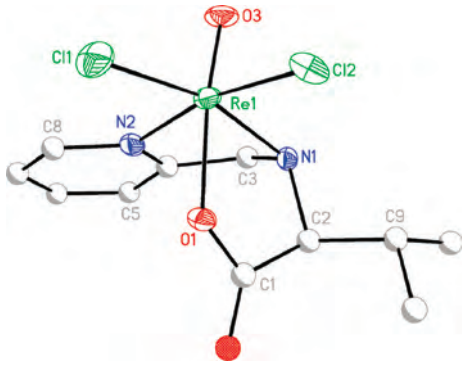

Figure 1. ORTEP plot and atom labeling scheme of $[Re^{V}O(L_A^1)Cl_2]$. All non-hydrogen atoms are represented by their 30% thermal probability ellipsoids.

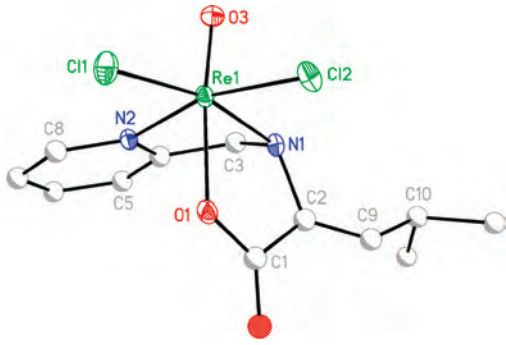

Figure 2. ORTEP plot and atom labeling scheme of $[Re^{V}O(L_A^2)Cl_2]$. All non-hydrogen atoms are represented by their 30% thermal probability ellipsoids.

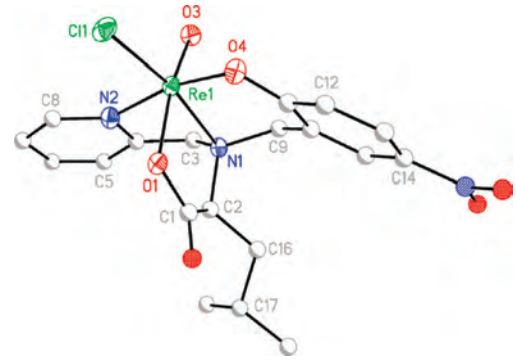

Figure 3. ORTEP plot and atom labeling scheme of $[Re^{V}O(L_B^2)Cl]$. All non-hydrogen atoms are represented by their 30% thermal probability ellipsoids.

corresponding atoms in molecules 1 and 2 are respectively *n* and *n* + 50, for example, Re1−O2 and Re51−O52.

$[Re^{V}O(L_A^1)Cl_2]$, 1a, and $[Re^{V}O(L_A^2)Cl_2]$, 1b. In both cases, the ligands bind as a facial coordination mode in which the carboxylate group occupies the axial position trans to the oxo oxygen atom. In a distorted octahedral geometry, the equatorial plane is made by two nitrogen atoms (N1 and N2) of the tridentate ligand, and the other two positions are occupied by chloro groups with a cis configuration. The short Re1−O3 bond distance in **1a** and **1b** is consistent with the multiple bond (Re═O).[35]

In the complexes, the $Re-O_{carboxylate}$ bond length is found to ∼2.02 Å, while the Re−N and Re−Cl bond distances fall in the range 2.11−2.17 Å and 2.31−2.37 Å, respectively.

$[Re^{V}O(L_B^2)Cl]$, 2b. The geometry of the complex appears to be distorted octahedral and characterized by an O═Re−O angle of 166.2(3), significantly deviated from the value of 180°. In the complex, the equatorial plane is occupied by a chloro group, two nitrogen atoms, and a phenoxide group of the tetradentate ligand part, while the carboxylate group of the ligand laid trans to the oxo oxygen atom, forming a distorted octahedral geometry. A short Re1−O4 was observed at 1.993(3) Å. The $Re-O_{carboxylate}$, Re−N, and Re−Cl bond distances are similar to those of **1a** and **1b**. The $Re-O_{phenoxide}$ bond distance is also usual.

The oxorhenium(V) complex with bis phenol containing O_2N_2-donating ligands and only one isomeric product (**I**) was obtained.[36a] It is documented that the hard donor site of the ligand occupies the position trans to the oxo oxygen atom, and this is due to the strong trans influence of the $Re{=}O^{3+}$ core.[36b−d] By considering the donating capability of phenoxide and the carboxylate group, isomer **III** is more likely to be formed. It is known that meridonially coordinated

(35) (a) Das, S.; Chakraborty, I.; Chakravorty, A *Inorg. Chem.* **2003**, *42*, 6545. (b) Chakroborty, I.; Bhattacharyya, S.; Banerjee, S.; Dirghangi, B. K.; Chakravorty, A. *J. Chem. Soc., Dalton Trans.* **1999**, 3747. (c) Edwards, P. J.; Griffith, W. P.; White, A. J. P.; Williams, D. J. *J. Chem. Soc., Dalton Trans.* **1992**, 957. (d) Mayer, J. M. *Inorg. Chem.* **1988**, *27*, 3899.

(36) (a) Mondal, A.; Sarkar, S.; Chopra, D.; Guru Row, T. N.; Rajak, K. K. *J. Chem. Soc., Dalton Trans.* **2004**, 3244. (b) Benny, P. D.; Barnes, C. L.; Piekarski, P. M.; Lydon, J. D.; Jurisson, S. S. *Inorg. Chem.* **2003**, *42*, 6519. (c) Bommen van, K. J. C.; Verboom, W.; Hulst, R.; Kooijman, H.; Spek, A. L.; Reinhoudt, D. N. *Inorg. Chem.* **2000**, *39*, 4099. (d) Herrmann, W. A.; Rauch, M. U.; Artus, G. R. J. *Inorg. Chem.* **1996**, *35*, 1988.

Scheme 1

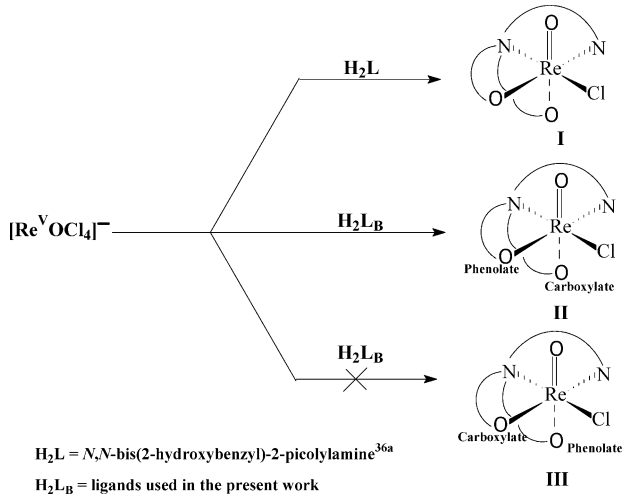

N-salicylidene α amino acidato oxovanadium complexes may exist in two diastereomeric forms, endo and exo.[34b,37] However, in most cases, the more stable endo form was observed in the solid state.[37] Therefore, at least the formation of the endo form of isomer **III** of oxorhenium complexes is expected (Scheme 1).

Interestingly, only isomer **II** is isolated exclusively in the solid state, where the carboxylate occupies the position trans to the Re═O moiety. The binding of the carboxylate group to the trans position is not well understood; however, it is believed that the R group gets more open space and exerts virtually no steric repulsion with the oxo oxygen or the remaining ligand part in isomer **II** over **III**, which favors the formation of the observed diastereoisomer.

We have also performed the geometry optimization in the gas phase of isomer **III** (Figure S1, in the Supporting Information) to compare the energy with that of the observed isomer **II**. It was found from the gas-phase optimization that isomer **II** is energetically more stable by 10 kcal/mol than **III**, which is in good agreement with the presence of isomer **II** in the crystal.

Geometry and Electronic Structure. The complexes are diamagnetic; thus, the geometry optimizations of three complexes were done in their singlet spin state. The molecular structures of $[Re^{V}O(L_A{}^1)Cl_2]$, $[Re^{V}O(L_A{}^2)Cl_2]$, and $[Re^{V}O(L_B{}^2)Cl]$ have been fully optimized in their singlet spin states. The calculated geometrical parameters involving the central rhenium atom is compared in Table 3 with the corresponding experimental values (detailed bond distances and angles are given the Supporting Information, Tables S2 and S3). The calculated bond distances are slightly deviated from the crystal structure parameters, with the largest discrepancies (0.09 Å) corresponding to the Re−N bond. In the calculated structures, some deviations in the bond angles are also observed. Although there are some discrepancies, the trends in distances and angles in the optimized gas-phase geometries obtained from the DFT level of calculations resemble with the X-ray structures.

The schematic molecular orbital energy diagrams from HOMO-5 to LUMO+5 of **1a**, **1b**, and **2b** are shown in Figure 4. The isodensity plots from HOMO-3 to LUMO+3 for **1a** and **2b** are shown in Figure 5a and b, respectively (HOMO-4 and HOMO-5 and LUMO+4 and LUMO+5 for both **1a** and **2b**; for complex **1b**, for HOMO-5 to LUMO+5, see the Supporting Information, Figures S2, S3, and S4, respectively). In complex **1a**, the HOMO may be characterized by the antibonding combination of the Re d_{xy} orbital (∼45%) and the p orbitals of chlorine (∼30%). HOMO-1 and HOMO-2 are lying ∼1.36 and ∼1.54 eV below, respectively, the HOMO. HOMO-1 orbitals mainly originate from the p orbitals of the chloro group (90%), whereas in HOMO-2, the electron density is delocalized between chlorine (50%), the oxo oxygen (10%), and the carboxylate group (20%). In the case of HOMO-3, the electron density mainly delocalized over chlorine and the amino acid residue.

LUMO+1 and LUMO+2 are lying 0.56 and ∼0.75 eV, respectively, above the LUMO. The electron densities of LUMO, LUMO+1, and LUMO+2 are mainly distributed between the metal d orbitals and the ligand frame. LUMO+3 is completely delocalized over the pyridine ring.

In complex **2b**, the HOMO is mainly composed of ∼58% Re_{dyz} orbitals and 25% chlorine p orbitals. HOMO-1 lies ∼0.53 eV below the HOMO and has no bonding/interaction with the central metal atom Re and the total electron density localized on the phenyl ring bearing phenoxide oxygen in the tetradentate ligand. In addition, HOMO-2 and HOMO-3 are found ∼ 1.40 and 1.56 eV below the HOMO, delocalized on the ring containing the $-NO_2$ group with a minor contribution from the amino acid residue and chlorine. LUMO is delocalized on the pyridine ring and the central Re atom, having contributions of 48% and 40%, respectively. LUMO+1 and LUMO+2 are almost degenerate, lying 0.50 and 0.65 eV above the LUMO. LUMO+1 shows main contributions from Re (∼60%) and chlorine (∼10%). LUMO+2 and LUMO+3 are completely delocalized over the ligand with a minor contribution of Re_d orbitals.

NMR Spectra. All of the complexes are diamagnetic in nature. ^1H and ^{13}C spectra of the complexes were performed and show well-resolved spectra in solution. The NMR spectra were assigned by considering chemical shift values, spin−spin intensity, and spin−spin-coupling patterns. The complexes display a well-resolved doublet around 9.50 ppm ($J = 5-7$ Hz) for **1** and 9.75 ppm for **2**, which correspond to the ortho

Table 3. Comparison of Calculated and Experimental Bond Distance [Å] and trans Angles [deg] for Complexes **1a**, **1b**, and **2b**

parameters	**1a**		1b		**2b**	
distance	calc.	exp.	calc.	exp.	calc.	exp.
Re═O	1.688	1.685	1.688	1.646	1.696	1.674
Re−O	2.023	2.019	2.023	2.020	2.002−2.034	1.993−2.001
Re−N	2.179−2.249	2.136−2.176	2.176−2.247	2.098−2.140	2.148−2.202	2.111−2.169
Re−Cl	2.362−2.385	2.319−2.342	2.363−2.384	2.328−2.367	2.366	2.341

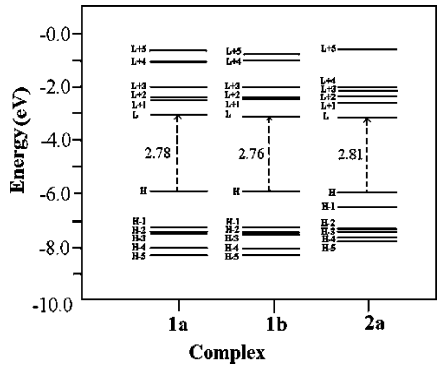

Figure 4. Schematic molecular orbital energy diagram for six occupied (H) and six virtual (L) frontier orbitals of the complexes in the singlet ground state (H = HOMO, L = LUMO).

proton of the pyridyl group. In solution, the −N*H* proton signal was observed at ∼5.0 ppm, which disappears upon shaking with D_2O. The α hydrogen atom of the amino acid residue occurs as an ill-resolved multiplet.

The resonances of inequivalent benzylic protons in the ligand frame were assigned individually on the basis of multiplicity and *J* values obtained as a strongly coupled doublet (14−17 Hz). It is clear from the X-ray crystal structure that one of the benzylic protons, H_A3, for complex **1**, and H_A3 and H_A9 for complex **2** in the ligand frame occupy the endo face with a Re═O core and the others (H_B3; H_B3 and H_B9) are on the exo side. The endo proton becomes more deshielded than the exo proton, resulting in a downfield shift of the signals, and the origin of the deshielding can be attributed to the anisotropic effect of the Re═O bond.[5b,38] The coordination of pyridyl nitrogen causes the low field shift of H3 atoms versus H9 atoms in the case of the $[Re^{V}O(L_B)Cl]$ complexes. A representative ^1H spectrum of **2b** is shown in Figure 6.

^{13}C NMR spectra of the complexes were also recorded, and the assigned peaks are given in the Experimental Section. The carboxylate carbon was observed in the region 180−175 ppm. For complex $[Re^{V}O(L_B)Cl]$, the carbon-bearing $-NO_2$ group and the phenolate carbon resonances occur in the regions 150−145 and 174−170 ppm, respectively. It is to be noted that there is no diastereoisomeric splitting of any of the ^1H and ^{13}C resonances either in the spectra.

In the present study, we have calculated the GIAO chemical shift and $^1H-^1H$ coupling constant for three molecules. The discrepancies between experimental and calculated values are lower than 0.80 and 4−6 ppm for the ^1H and ^{13}C chemical shifts, respectively.

The calculated spin−spin coupling constant values are also satisfactorily displaying an error of about 0.7 Hz. However, the pattern of experimentally observed spectra is retained in calculated spectra (Supporting Information Table S4; Experimental Section).

The experimentally observed values are well-correlated with calculated values. The correlation diagram between the calculated (in solvent) and experimental ^{13}C chemical shift is given in the Supporting Information (Figure S5), and $^nJ_{H,H}$ coupling constants for complex **1a** and **2b** are given in Figure 7.

Thus, in summary, it may be concluded that the gross geometry of the molecule remains unaltered in solution.

Absorption and CD Spectra. The absorption spectra of the complexes were recorded in acetonitrile solution. Circular dichroism generally gives more useful information to elucidate the structural conformation of chiral complexes Therefore, the CD spectra (600−200 nm) were also performed in acetonitrile. The position of bands and the corresponding ε values are given in the Experimental Section. Figure 8a includes the absorption and CD spectra in the UV region for complex **1a**.

The complexes display one band in the visible region and three bands in the UV region. In the visible region absorption spectra, a broad band appears near 690 nm. This transition is logically assigned as ligand field excitation.[39] All of the absorption bands in the UV region are circularly dichroic in nature. For $[Re^{V}O(L_B)Cl]$ complexes, the absorption bands at ∼350 and ∼275 nm are observed at ∼365 and ∼280 nm in the CD spectra with a negative cotton effect.

The bands are believed to be of ligand-to-metal charge-transfer transition (LMCT) and $\pi-\pi^*$ transition, respectively.[36a,39b,c] The CD spectral band at 220 nm with a positive cotton effect is recognized as a characteristic band for the L-absolute configuration of α amino acids originating from the $n-\pi^*$ transition of the carboxylic group.[40]

$[Re^{V}O(L_A)Cl_2]$ species possess a similar absorption spectral pattern; however, there are dissimilarities in the CD spectra. In the case of $[Re^{V}O(L_A)Cl_2]$, the $\pi-\pi^*$ band occurs with a positive cotton effect.

The Figure 8b illustrates the calculated spectrum for complex $[Re^{V}O(L_A{}^1)Cl_2]$. Table 4 provides information on the calculated excitation energy, oscillator strength, and main configurational contribution toward excitation (for $[Re^{V}O(L_A{}^2)Cl_2]$, see the Supporting Information, Table S5). The bands appeared in the computed spectra ∼0.15 eV blue-shifted with respect to the experimental value. The absorption calculated at 680 nm can be unambiguously related to the experimental band at ∼700 nm and arising from HOMO → LUMO+1. Therefore, this band can be assigned to the classical d−d transition. The calculated CD band with a negative cotton effect at 350 nm arises from the absorption band at 337 nm. The band centered at 337 nm appears to be

(37) Rajak, K. K.; Baruah, B.; Rath, S. P.; Chakravorty, A. *Inorg. Chem.* **2000**, *39*, 1598.
(38) (a) Hansen, L.; Hirota, S.; Xu, X. ; Taylor, A. T.; Marzilli, L. G. *Inorg. Chem.* **2000**, *39*, 5731. (b) Hansen, L.; Xu, X.; Lipowska, M.; Taylor, A.; Marzilli, L. G. *Inorg. Chem.* **1999**, *38*, 2890. (c) Hansen, L.; Xu, X.; Yue, K. T.; Taylor, A, Jr.; Marzilli, L. G. *Inorg. Chem.* **1996**, *35*, 2785. (d) Papadopoulos, M. S.; Pirmettis, I. C.; Pelecanou, M.; Raptopoulou, C. P.; Terzis, A.; Stassinopoulou, C. I.; Chiotellis, E. *Inorg. Chem.* **1996**, *35*, 7377. (e) Papadopoulos, M. S.; Pirmettis, I. C.; Pelecanou, M.; Raptopoulou, C. P.; Terzis, A.; Stassinopoulou, C. I.; Chiotellis, E. *Inorg. Chem.* **1996**, *35*, 4478. (f) Oneil, J. P.; Wilson, S. R.; Katzenellenbogen, J. A. *Inorg. Chem.* **1994**, *37*, 319.
(39) (a) Dirghangi, B. K.; Menon, M.; Pramanik, A.; Chakravorty, A. *Inorg. Chem.* **1997**, *36*, 1095. (b) Bereau, V. M.; Khan, S. I.; Abu-Omar, M. M. *Inorg. Chem.* **2001**, *40*, 6767. (c) Tisato, F.; Refosco, F.; Mazzi, U.; Bandoli, G.; Nicolini, M. *J. Chem. Soc., Dalton Trans.* **1987**, 1693.
(40) (a) Fowden, L.; Scopes, P. M.; Thomas, R. N. *J. Chem. Soc. C* **1971**, 833. (b) Legrand, M.; Viennet, R. *Bull. Soc. Chim. Fr.* **1965**, 679.

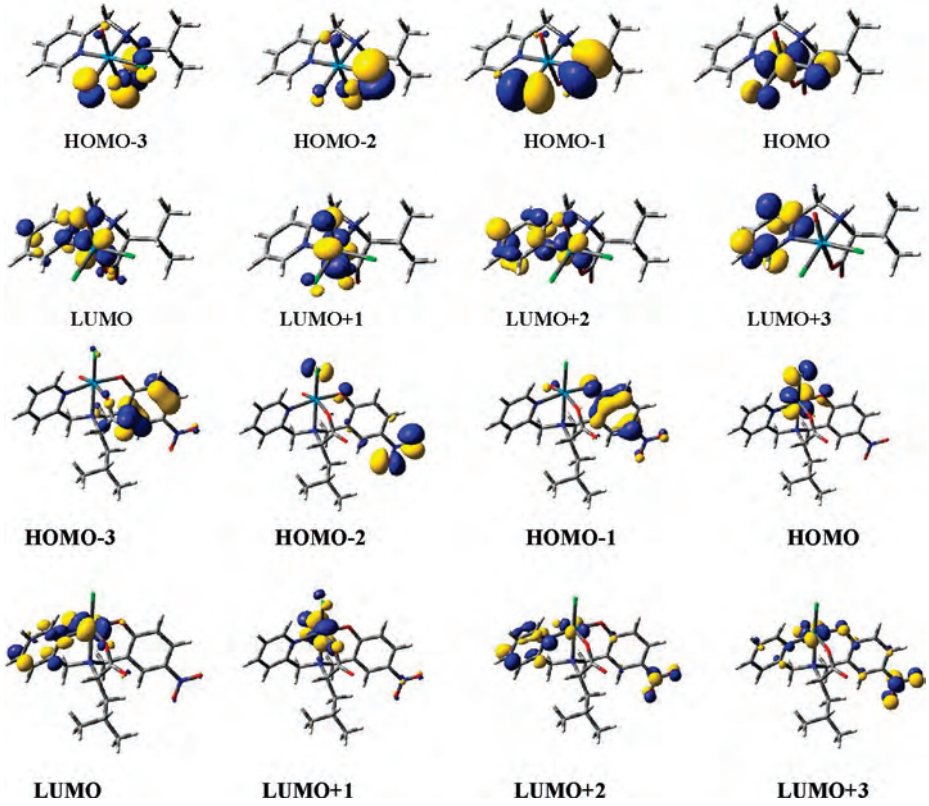

Figure 5. (a, top two rows) Isodensity plots of frontier orbitals of $[Re^{V}O(L_A{}^1)Cl_2]$. (b, bottom two rows) Isodensity plots of frontier orbitals of $[Re^{V}O(L_B{}^2)Cl]$.

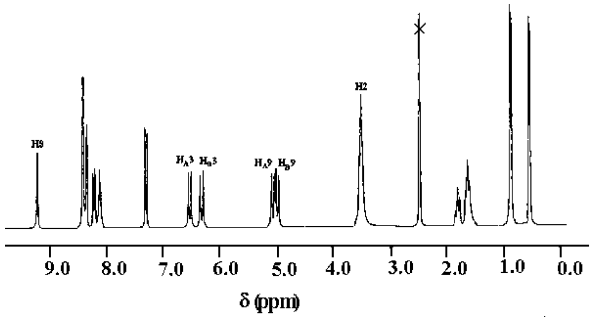

Figure 6. ^{1}H NMR spectrum of $[Re^{V}O(L_B{}^2)Cl]$ in DMSO-d_6 solution.

a composition of four main transitions and this excitation dominated by HOMO-3 → LUMO, HOMO-2 → LUMO, HOMO-1 → LUMO, and HOMO → LUMO+3 transitions. Thus, this excitation is believed to be of LMCT transition. The intense CD band with a positive cotton effect and absorption band occurring at ∼280 nm can be attributed to a ligand $\pi-\pi^*$ transition originating from HOMO-6 → LUMO, HOMO-5 → LUMO, HOMO-5 → LUMO+1, HOMO-3 → LUMO+1, and HOMO-2 → LUMO+1 excitations.

The L-absolute configuration of amino acid is obtained in the calculated CD spectra at 217 nm with a positive cotton effect, and major excitations contributing to the absorption band at 218 nm are HOMO-10 → LUMO+1, HOMO-4 → LUMO+2, HOMO-3 → LUMO+4, HOMO-2 → LUMO+4, and HOMO-1 → LUMO+4 transitions.

Table S6 (Supporting Information) provides information on the calculated excitation energy, oscillator strength, and main configurational contribution toward the excitation of

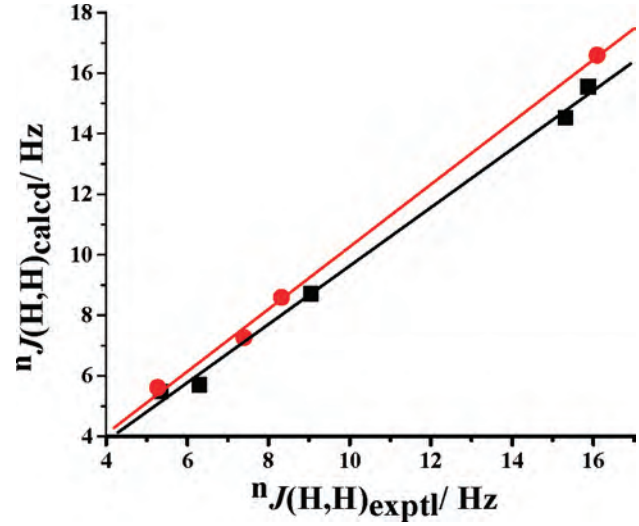

Figure 7. Linear correlation between the experimental and calculated ^nJ(H,H) of **1a** (●) and **2b** (■).

$[Re^{V}O(L_B{}^2)Cl]$. The calculated spectra are observed ∼0.10 eV blue-shifted compared to that of the experimental values, and the d−d transition appears at 685 nm for absorption. The LMCT features of the complex are calculated at 352 nm in the absorption spectra and 360 nm in the CD spectra with a negative cotton effect. The theoretical absorption spectra exhibits $\pi-\pi^*$ transition at 280 nm (275 nm in CD spectra) with a negative cotton effect.

In summary, both the calculated and experimental spectral studies demonstrate that all of the synthesized

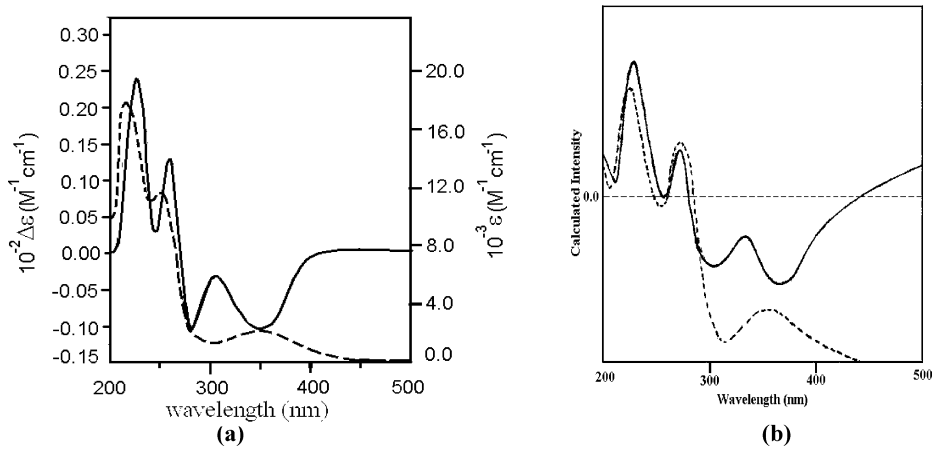

Figure 8. (a) Experimental and (b) computed UV−vis absorption (---) and CD (—) spectra of complex **1a** in acetonitrile solution.

Table 4. Main Calculated Optical Transition for Complex **1a** with Composition in Terms of Molecular Orbital Contribution of the Transition, Vertical Excitation Energies, and Oscillator Strength in Acetonitrile

excitation	composition	*E* (eV)	oscillator strength (f)	λ_{Theo}(nm)	λ_{exp}(nm)
1	HOMO → LUMO+1 (95%)	1.81	0.0005	684.6	700
2	HOMO-3 → LUMO (70%) HOMO-2 → LUMO (30%)	3.55	0.0025	349.4	352
3	HOMO-3 → LUMO (60%) HOMO-1 → LUMO (25%) HOMO → LUMO+2 (15%)	3.67	0.0091	338.4	
4	HOMO-3 → LUMO (24%) HOMO-1 → LUMO (47%) HOMO → LUMO+2 (25%)	3.68	0.0038	337.0	
5	HOMO-3 → LUMO (48%) HOMO-2 → LUMO (24%) HOMO-1 → LUMO (27%)	3.81	0.0074	325.1	
6	HOMO-6 → LUMO (16%) HOMO-5 → LUMO (30%) HOMO-4 → LUMO+1 (14%) HOMO-3 → LUMO+1 (22%) HOMO-2 → LUMO+1 (10%) HOMO-1 → LUMO+1 (7%)	4.19	0.0276	295.7	280
7	HOMO-6 → LUMO (7%) HOMO-5 → LUMO (10%) HOMO-4 → LUMO+1 (14%) HOMO-3 → LUMO+1 (30%) HOMO-2 → LUMO+1 (29%) HOMO-1 → LUMO+1 (8%)	4.22	0.0222	293.3	
8	HOMO-8 → LUMO (13%) HOMO-8 → LUMO+1 (7%) HOMO-7 → LUMO (7%) HOMO-6 → LUMO (36%) HOMO-6 → LUMO+1 (8%) HOMO-5 → LUMO (25%)	4.32	0.0241	286.8	
9	HOMO-10 → LUMO (8%) HOMO-9 → LUMO+1 (7%) HOMO-8 → LUMO (10%) HOMO-7 → LUMO (32%) HOMO-6 → LUMO (10%) HOMO-6 → LUMO+1 (8%) HOMO-5 → LUMO+1 (22%)	4.66	0.0234	266.2	
10	HOMO-3 → LUMO+4 (30%) HOMO-2 → LUMO+4 (60%)	5.61	0.0313	220.8	215
11	HOMO-4 → LUMO+2 (90%)	5.69	0.0298	218.1	
12	HOMO-13 → LUMO+6 (12%) HOMO-13 → LUMO+1 (15%) HOMO-11 → LUMO+1 (20%) HOMO-10 → LUMO+1 (14%) HOMO-9 → LUMO+1 (18%) HOMO-1 → LUMO+4 (20%)	5.76	0.0240	214.9	

oxorhenium(V) complexes exist in enantiomeric pure form in solution, retaining the L-absolute configuration of α amino acids.

Electrochemistry. The cyclic voltammogram was recorded in an acetonitrile solution using platinum as a working electrode versus SCE. (The representative spectra of **1a** and

2b are given in the Supporting Information, Figure S7.) Upon scanning to positive potential, the $[Re^{V}O(L_A)Cl_2]$ and $[Re^{V}O(L_B)Cl]$ complexes exhibited an irreversible and quasireversible response at ~1.40 and ~1.50 V, respectively. This redox process is assigned to the $Re^{V/VI}$ oxidation couple.[3] It appears that, for the $[Re^{V}O(L_B)Cl]$ complexes, the oxidized species is stable at least on the voltammetric time scale compared to that of the oxidized congener of $[Re^{V}O(L_A)Cl_2]$ complexes. It is believed that the strong σ-donating nature of the N_2O_2 ligand is responsible for the stability of the hexavalent state of rhenium. The cathodic shift of $[Re^{V}O(L_A)Cl_2]$ complexes by 100 mV compared to $[Re^{V}O(L_B)Cl]$ can be attributed to the destabilization of the HOMO of the $[Re^{V}O(L_A)Cl_2]$. In the present case, the electrochemical behavior of the complexes is consistent with the other reported oxorhenium(V) complexes using O_2N and N_2O_2 flexible ligands.[36a]

Conclusion

NNO and NONO coordinating flexible ligands bearing chiral α amino acids (L-valine, L-leucine, and L-phenylalanine) have been utilized to generate oxorhenium(V) complexes. The complexes are isolated in enantiomeric pure form, revealed by X-ray structure determination. The species represented herein describe the structurally characterized chiral oxorhenium(V) complexes incorporating conformationally labile NNO and NONO coordinating ligands derived from L amino acids. NMR (^1H and ^{13}C) and CD spectral studies have demonstrated that no isomerization is observed in solution.

To provide better insight into the properties of their ground state and excited states, detailed calculations of $[Re^{V}O(L_A^1)Cl_2]$, $[Re^{V}O(L_A^2)Cl_2]$, and $[Re^{V}O(L_B^2)Cl]$ were performed at the DFT level. The optimized geometric parameters in the ground state are in good agreement with experimental measured values. The DFT calculation also supports the formation of diastereoisomer **II**.

The computed absorption and CD spectra for the three complexes in the UV−vis region were assigned by the TDDFT approach combined with the CPCM solvent model. The calculations predict that the lowest-lying transition is due to d−d excitation, while that of the 400−280 nm region is associated with LMCT and ligand-to-ligand charge transfer excitation. The calculated NMR spectral data are satisfactory when compared with the experimental values.

Our search for new rhenium complexes in various oxidation states with polydentate ligands containing amino acids and peptides and their characterization by different theoretical models is continuing.

Acknowledgment. Financial support from the University Grant Commission, New Delhi, India, Council of Scientific and Industrial Research, New Delhi, India, and Department of Science and Technology, New Delhi, India is greatly acknowledged. We are also thankful to the School of Chemistry, Hyderabad University, India and the Department of Chemistry, Indian Institute of Technology, Guwahati, India for the data collection on the CCD facility setup.

Supporting Information Available: Calculated bond distances and angles; isodensity plots of frontier orbitals for **1a**, **1b**, and **2b**; optimized structure of isomer **III**; correlation diagrams of ^{13}C chemical shifts; calculated vertical excitation energies and oscillator strength of **1b** and **2b**; and cyclic voltammograms of **1a** and **2b** (PDF). X-Ray crystallographic files in CIF format for $[Re^{V}O(L_A^1)Cl_2]$, $[Re^{V}O(L_A^2)Cl_2]$, and $[Re^{V}O(L_B^2)Cl]$. This material is available free of charge via the Internet at http://pubs.acs.org.

IC800764N